IOP Conf. Series: Journal of Physics: Conf. Series **876** (2017) 012022 doi:10.1088/1742-6596/876/1/012022

TDA and RPA pseudoscalar and vector solutions for the low energy regime of a motivated QCD Hamiltonian.

T. Yépez-Martínez[1], D. A. Amor Quiroz[2], P. O. Hess[2] and O. Civitarese[1]

[1] Departamento de Física, Universidad Nacional de La Plata, C.C.67 (1900), La Plata, Argentina

[2] Instituto de Ciencias Nucleares, UNAM, Circuito Exterior, C.U., A.P. 70-543, 04510 México, D.F., México.

E-mail: yepez@fisica.unlp.edu.ar, arturo.amor@nucleares.unam.mx, hess@nucleares.unam.mx, osvaldo.civitarese@fisica.unlp.edu.ar

Abstract. We present the low energy meson spectrum of a Coulomb gauge QCD motivated Hamiltonian for light and strange quarks. We have used the harmonic oscillator as a trial basis and performed a pre-diagonalization of the kinetic energy term in order to get an effective basis where quark and anti-quark degrees of freedom are defined. For the relevant interactions between quarks and anti-quarks, we have implemented a confining interaction between color sources, in order to account in an effective way for the gluonic degrees of freedom. The low energy meson spectrum is obtained from the implementation of the TDA and RPA many-body-methods. The physical states have been described as TDA and RPA collective states with a relatively good agreement. Particularly, the particle-hole correlations of the RPA ground state improve the RPA pion-like state (159.7 MeV) close to its physical value while the TDA one remains at a higher energy (269.2 MeV).

1. Introduction

The Quantum Chromodynamics (QCD) is the fundamental theory of strong interaction, the basic ingredients of this theory are the elementary particles, quarks and gluons. The QCD describes the propagation and interactions of these particles. The quarks and gluons are color charged particles, where due to the non-abelian nature of the theory, the gluons can interact with themselves. The latter is a very important characteristic since several interactions and phenomena are associated to this fact, *e.g.*, the confinement of quarks and the chiral symmetry breaking. The low energy regime of QCD is highly non-perturbative since the interaction coupling is large. However, the Lattice Gauge Theory (LGT) [1–4], the Dyson-Schwinger equation (DS-eq) [5–7] and the effective models [8–11] have been able to get some insights about this regime. Particularly, the determination of the spectrum of QCD at low energy has been a task for many years. In dealing with this problem, LGT has shown to be a very powerful tool. Unfortunately, it has several disadvantages like huge computational efforts, problems with the identification of the states with a given spin and the calculation of excited states. Recently, LGT has been able to determine the spectrum of light and more heavy [3,4] quarks in relatively

good agreement with the available experimental data.

From the side of the phenomenological approaches, to work with an effective interaction has shown to be also a good tool in order to describe the spectrum at low energy. They can be questionable mainly because the origin of the interactions and how they are related to real QCD. The Coulomb gauge QCD formalism derived in [12], underlying the relevant interactions of QCD which are dominated by the instantaneous Coulomb potential (ICP) acting between color charges. It is known that a confinement interaction able to reproduce LGT potential results [13], can be obtained in this formalism by the implementation of self-consistent treatments like DS-eq in the Yang-Mills sector and under certain approximations of the vacuum functional of QCD [14–16]. Following that direction, we have focused on the quark sector of the Coulomb gauge QCD Hamiltonian and accounts for the effects of the gluon dynamics with an effective interaction. In the past, we have analysed, step by step, the implementation of a parametrized interaction with analytic and semi-analytic approaches as well as pairing methods like BCS [17, 18]. More recently, we have implemented the Tamm-Dancoff-Approximation (TDA) [19, 20] and the Random-Phase-Approximation (RPA) [21, 22] many-body methods, in order to describe meson states as collective states.

In this work, we have considered a more realistic interaction of the type Coulomb ($-a/|\mathbf{x}-\mathbf{y}|$) plus linear ($b|\mathbf{x}-\mathbf{y}|$) potential and implement both the TDA and RPA methods [23]. We have restricted the calculations to well defined sub-spaces of spin, parity (J^P), flavor-hypercharge and isospin (Y, T) and only color-singlet $(0,0)_1$ or physical states. Within these sub-spaces, we have analyzed two sets of parameters, where the quark masses and interaction parameter were adjusted in order to reproduce certain features of the low lying meson spectrum. Particularly, the set of parameters leading to a RPA-pion-like state close to the experimental value is used for comparison with other similar approaches [24] and with experimental data [25] .

2. Motivated QCD Hamiltonian and basic ingredients.

We consider a motivated QCD Hamiltonian which is built by the kinetic and mass terms together with a confining interaction between quark color charge densities,

$$H_{eff} = \int \left\{\psi^\dagger(\mathbf{x})(-i\alpha\cdot\nabla + \beta m_0)\psi(\mathbf{x})\right\} d\mathbf{x} - \frac{1}{2}\int \rho_a(\mathbf{x})V(|\mathbf{x}-\mathbf{y}|)\rho^a(\mathbf{y})d\mathbf{x}d\mathbf{y}, \tag{1}$$

where $\rho^a(\mathbf{x}) = \rho^a_q(\mathbf{x}) = \psi^\dagger(\mathbf{x})T^a\psi(\mathbf{x})$ and

$$\begin{aligned}\psi^\dagger(\mathbf{x}) &= \sum_{\tau N l m_l \sigma c f} R^*_{Nl}(x)Y^*_{lm_l}(\widehat{\mathbf{x}})\chi^\dagger_\sigma \mathbf{b}^\dagger_{\tau,Nlm_l,\sigma cf} \\ &= \sum_{Njm_j lm_l,\sigma cf} R^*_{Nl}(x)\langle lm_l,\frac{1}{2}\sigma|jm_j\rangle Y_{lm_l}(\hat{\mathbf{x}})\chi^\dagger_\sigma \left(b^\dagger_{-\frac{1}{2}(Nl)jm_j,cf} + b^\dagger_{\frac{1}{2}(Nl)jm_j,cf}\right) . \end{aligned} \tag{2}$$

In the last step, we have used the coupled representation of angular momentum and intrinsic spin-$\frac{1}{2}$ to total spin (j). The index τ identifies the creation(annihilation) of particles with positive $\tau = \frac{1}{2}$ and negative energy $\tau = -\frac{1}{2}$. The color and flavor intrinsic degrees of freedom are denoted by c and f, where f is a short hand notation for flavor hypercharge, isospin and third component of isospin $\{Y, T, T_z\}$. Since we are going to consider that the chiral and flavor symmetries are broken ($m_0 \neq 0$ and $m_0 \to m_0^T$), the mass of the light up and down ($T = \frac{1}{2}$) quarks are different than the strange ($T = 0$) quark ($m_{u,d} \neq m_s$).

Because of confinement, the domain of fields in Eq. (2) is expected to be restricted to a finite volume in space. Therefore, the eigenfunctions of the three dimensional harmonic oscillator are chosen as the single-particle orbitals.

$$R_{Nl}(x) = N_{Nl}\exp(-\frac{B_0x^2}{2})r^l L^{l+\frac{1}{2}}_{\frac{N-l}{2}}(B_0x^2) , \tag{3}$$

where N refers to the number of oscillation-quanta of the orbital level and l the angular momentum. The particles are restricted to a finite volume of the size of the oscillator length ($\frac{1}{\sqrt{B_0}}$).

The use of the harmonic oscillator basis for the orbital part seems to restrict the validity of the approximations to a non-relativistic theory, but this is only true when individual levels are considered to describe quark states. When the complete basis is used, any relativistic state can be expanded into the non-relativistic basis. This requires to expand the relativistic states into, in general, an infinite sum. When sufficient basis states are included, this sum can be limited in such a way that adding new terms would not modify the results. The latter is related with a non-trivial renormalization procedure [22]. Here, we explore the low energy meson spectrum in terms of the basic ingredients.

2.1. The Hamiltonian matrix elements.
Using the fermion field quatization given in Eq. (2), the Hamiltonian of Eq. (1) is expressed as

$$\begin{aligned} H_{eff} &= \sum_{jT}\sum_{\tau_i N_i l_i} K^{j,T}_{\tau_1(N_1l_1),\tau_2(N_2l_2)} \left(\boldsymbol{b}^{\dagger}_{\tau_1(N_1,l_1)jT}\cdot \boldsymbol{b}^{\tau_2(N_2,l_2)jT}\right) \\ &+ \sum_{\{N_i l_i j_i;L\}} V^{L}_{\{N_i l_i j_i\}} \left[\left[b^{\dagger}_{(N_1l_1)j_1T_1}\otimes b_{(N_2l_2)j_2T_2}\right]^{\gamma}\otimes\left[b^{\dagger}_{(N_3l_3)j_3T_3}\otimes b_{(N_1l_1)j_4T_4}\right]^{\gamma}\right]^{\hat{0}} \end{aligned} \tag{4}$$

where $\gamma = 0, L, (1,1)_1, 0, 0$ indicates the intermediate couplings of pseudo-spin, spin ($L = 0, 1$), $(1,1)_1$-color and flavor hypercharge and isospin quantum numbers. The scalar structure of the interaction is denoted by $\hat{0} = 0, (0,0)_1, 0$, representing the total spin, color and flavor hypercharge and isospin couplings.

The matrix elements of the kinetic-energy are given by

$$K^{j,T}_{\tau_1(N_1l_1),\tau_2(N_2l_2)} = \begin{cases} k^{j}_{N_1N_2} & \text{if } l_1 = j+\frac{1}{2}\ ,\ l_2 = j-\frac{1}{2}\ ,\ \tau_1 \neq \tau_2 \\ k^{j}_{N_2N_1} & \text{if } l_1 = j-\frac{1}{2}\ ,\ l_2 = j+\frac{1}{2}\ ,\ \tau_1 \neq \tau_2 \\ m_0^T & \text{if } (N_1l_1) = (N_2l_2)\ ,\ \tau_1 = \tau_2 = +\frac{1}{2} \\ -m_0^T & \text{if } (N_1l_1) = (N_2l_2)\ ,\ \tau_1 = \tau_2 = -\frac{1}{2} \\ 0 & \text{in all other cases} \end{cases} \tag{5}$$

with $m_0^T = m_{u,d}\delta_{T,\frac{1}{2}} + m_s\delta_{T,0}$ and

$$k^{j}_{N_1N_2} = \sqrt{B_0}\sqrt{\frac{N_1 - j + \frac{3}{2}}{2}}\delta_{N_2,N_1+1} + \sqrt{B_0}\sqrt{\frac{N_1 + j + \frac{3}{2}}{2}}\delta_{N_2,N_1-1} \tag{6}$$

while the potential matrix elements are given by

$$\begin{aligned} &V^{L}_{\{N_i l_i j_i\}} \\ &= \sum_{JN_r'N_rl_rN_RL_R} 3\sqrt{8}\sqrt{(2j_1+1)(2j_2+1)(2j_3+1)(2j_4+1)}\sqrt{2L+1}(2J+1) \\ &\times(-1)^{L+j_2+j_4-J+1}\left\{\begin{array}{ccc} l_1 & L & l_2 \\ j_2 & \frac{1}{2} & j_1 \end{array}\right\}\left\{\begin{array}{ccc} l_3 & L & l_4 \\ j_4 & \frac{1}{2} & j_3 \end{array}\right\}\left\{\begin{array}{ccc} l_2 & J & l_4 \\ l_3 & L & l_1 \end{array}\right\} \\ &\times(N_r'l_r, N_RL_R, J \mid N_1l_1, N_3l_3, J)(N_rl_r, N_RL_R, J \mid N_2l_2, N_4l_4, J)\int d^3r\Psi^{*}_{N_r'l_r'l_r}(\mathbf{r})V(\sqrt{2}r)\Psi_{N_rl_rl_r}(\mathbf{r}) \quad . \end{aligned} \tag{7}$$

The potential $V(\sqrt{2}r)$ represents the confining potential in term of the relative coordinate $\mathbf{r} = \frac{1}{\sqrt{2}}(\mathbf{x} - \mathbf{y})$. In Eq. (7), we have used the Moshinsky brackets (round-brackets) [26, 27] and integrated the center of mass coordinate $\mathbf{R} = \frac{1}{\sqrt{2}}(\mathbf{x} + \mathbf{y})$. The detailed derivation can be found in [22].

3. The pre-diagonalization of the kinetic term and the effective basis.

The diagonalization of the kinetic term (Eq. (5)) is achieved by a general procedure *i.e.*, we implement a unitary basis transformation

$$\boldsymbol{b}^{\dagger}_{\tau(N,l)jm_jcTT_z} = \sum_{\lambda\pi k} \left(\alpha^{jT}_{\tau(N,l);\lambda\pi k}\right)^{*} \boldsymbol{b}^{\dagger}_{\lambda\pi kjm_jcTT_z} \tag{8}$$

where the kinetic term has a diagonal representation

$$\sum_{\tau_i,N_i,l_i} \left(\alpha^{j,T}_{\tau_1,(N_1,l_1),\lambda_1\pi_1k_1}\right)^{*} K^{j,T}_{\tau_1(N_1l_1),\tau_2(N_2l_2)} \alpha^{j,T}_{\tau_2,(N_2,l_2),\lambda_2\pi_2k_2} = \varepsilon_{\lambda_1,\pi_1,k_1,j,T}\ \delta_{\lambda_1,\lambda_2}\delta_{\pi_1,\pi_2}\delta_{k_1,k_2}\ . \tag{9}$$

The corresponding eigenvalues ($\varepsilon_{\lambda_1,\pi_1,k_1,j,T}$) and eigenvectors $\left(\alpha^{jT}_{\tau(N,l);\lambda\pi k}\right)$ allow us to rewrite the Hamiltonian in terms of creation(annihilation) effective $b^{\dagger}_{\Gamma_i}(b_{\Gamma_i})$ quarks ($\lambda_i = 1/2$) and $d^{\dagger}_{\Gamma_i}(d_{\Gamma_i})$ anti-quarks ($\lambda_i = -1/2$) operators:

$$\begin{aligned} H_{eff} &= \sum_{\pi,k,j,Y,T} \varepsilon_{\pi,k,j,Y,T}\Big(\boldsymbol{n}_{\pi,k,j,Y,T} + \bar{\boldsymbol{n}}_{\pi,k,j,Y,T}\Big) \\ &- \frac{1}{2}\sum_{L}\sum_{\{\gamma_i\}} V^{L}_{\{\gamma_i\}}\Big\{ \Big[\Big(\Big[\boldsymbol{b}^{\dagger}_{\gamma_1}\otimes\boldsymbol{b}_{\gamma_2}\Big]^{\gamma} - \Big[\boldsymbol{d}_{\gamma_1}\otimes\boldsymbol{d}^{\dagger}_{\gamma_2}\Big]^{\gamma}\Big)\otimes\Big(\Big[\boldsymbol{b}^{\dagger}_{\gamma_3}\otimes\boldsymbol{b}_{\gamma_4}\Big]^{\gamma} - \Big[\boldsymbol{d}_{\gamma_3}\otimes\boldsymbol{d}^{\dagger}_{\gamma_4}\Big]^{\gamma}\Big)\Big]^{\hat{0}} \\ &+ \Big[\Big([\boldsymbol{d}_{\gamma_1}\otimes\boldsymbol{b}_{\gamma_2}]^{\gamma} - \Big[\boldsymbol{b}^{\dagger}_{\gamma_1}\otimes\boldsymbol{d}^{\dagger}_{\gamma_2}\Big]^{\gamma}\Big)\otimes\Big([\boldsymbol{d}_{\gamma_3}\otimes\boldsymbol{b}_{\gamma_4}]^{\gamma} - \Big[\boldsymbol{b}^{\dagger}_{\gamma_3}\otimes\boldsymbol{d}^{\dagger}_{\gamma_4}\Big]^{\gamma}\Big)\Big]^{\hat{0}}\Big\} \end{aligned} \tag{10}$$

where $\boldsymbol{n}_{\pi,k,j,Y,T}$ and $\bar{\boldsymbol{n}}_{\pi,k,j,Y,T}$ are the quark and anti-quark number operators, $\gamma_i = \pi_i k_i j_i Y_i T_i$ and $V^{L}_{\{\gamma_i\}} = V^{L}_{\{\lambda_i,\pi_i,k_i,j_i,Y_i,T_i\}}$ with

$$\begin{aligned} V^{L}_{\{\lambda_i,\pi_i,k_i,j_i,Y_i,T_i\}} &= \sum_{\tau_i,N_i,l_i} V^{L}_{\{N_il_ij_i\}}\ \alpha^{j_1,T_1}_{\tau_1(N_1l_1),\lambda_1,\pi_1,k_1}\alpha^{j_2,T_2}_{\tau_2(N_2l_2),\lambda_2,\pi_2,k_2}\alpha^{j_3,T_3}_{\tau_3(N_3l_3),\lambda_3,\pi_3,k_3}\alpha^{j_4,T_4}_{\tau_4(N_4l_4),\lambda_4,\pi_4,k_4} \\ &\times\ \delta_{\tau_1\tau_2}\delta_{\tau_3\tau_4}\ (-1)^{\frac{1}{3}+\frac{Y_1}{2}+T_1}\frac{\sqrt{2T_1+1}}{\sqrt{3}}\delta_{T_2T_1}\delta_{Y_2-Y_1}\ (-1)^{\frac{1}{3}+\frac{Y_3}{2}+T_3}\frac{\sqrt{2T_3+1}}{\sqrt{3}}\delta_{T_4T_3}\delta_{Y_4-Y_3} \end{aligned} \tag{11}$$

The new extra factor $(-1)^{\frac{1}{3}+\frac{Y_1}{2}+T_1}\frac{\sqrt{2T_1+1}}{\sqrt{3}}\delta_{T_2T_1}\delta_{Y_2-Y_1}$ appears as a consecuence of the flavor symmetry breaking and it comes from extracting the flavor isoscalar of SU(3) [28]. In Eq. (10), all the information of the chiral and flavor symmetry breaking is carried by the coeficients $\alpha^{j,T}_{\tau(Nl),\lambda,\pi,k}$ of the unitary transformation Eq. (8).

4. The TDA and RPA pseudoscalar and vector solutions.

We implement the TDA and RPA methods [19–23], to define collective states as a linear combination of the pairs, built by quark ($b^{\dagger}_{\gamma_i}$) and anti-quark ($d^{\dagger}_{\gamma_i}$). The creation RPA collective

operator is given by

$$\hat{\Gamma}^{\dagger}_{n;\Gamma\mu} = \sum_{\gamma_a,\gamma_b} \left\{ X^{n}_{\gamma_a,\gamma_b;\Gamma}[b^{\dagger}_{\gamma_a} d^{\dagger}_{\gamma_b}]^{\Gamma}_{\mu} - Y^{n}_{\gamma_a,\gamma_b;\Gamma}(-1)^{\phi_{\Gamma\mu}}[d^{\gamma_b} b^{\gamma_a}]^{\Gamma}_{\bar{\mu}} \right\} \tag{12}$$

where we have used the short hand notation $\Gamma = J^P, (0,0)_1, Y, T$ to denote the spin-parity, color and flavor hypercharge and isospin of the collective operator and $\mu = M_J, 0, T_z$. The index n labels the new collective state and it runs from zero to the number of possibilities to form pairs with quantum numbers $\Gamma\mu$. The backward amplitudes $Y^{n}_{\gamma_a,\gamma_b;\Gamma} \neq 0$ imply the possibility of annihilate pairs from the ground state and in that sense the RPA method accounts for particle-hole correlations on both: the ground state and the excited states. The n-th RPA excited state is obtained by $|n;\Gamma\mu\rangle = \hat{\Gamma}^{\dagger}_{n;\Gamma\mu}|RPA\rangle$ and the RPA-ground-state ($|RPA\rangle$) is constructed in such a way that the condition $\hat{\Gamma}^{n;\Gamma\mu}|RPA\rangle = 0$ is fulfilled.

The TDA collective operator is obtained from the RPA one by setting to zero the backward amplitudes $Y^{n}_{\gamma_a,\gamma_b;\Gamma} = 0$. Thus, the n-th TDA excited state is obtained by $|n;\Gamma\mu\rangle = \hat{\Gamma}^{\dagger}_{n;\Gamma\mu}|\tilde{0}\rangle$, where the TDA-ground-state ($|\tilde{0}\rangle$) is annihilated by the quark and anti-quark operators $b_{\gamma_i}|\tilde{0}\rangle = d_{\gamma_i}|\tilde{0}\rangle = 0$.

In Table 1, we show how the subspaces defined by quantum numbers of the collective states $J^P, (0,0)_1, Y, T$ are related with the physical pseudoscalar and vector mesons. In particular, the subspaces with $Y, T = 0, 0$, do not show any flavor mixing between pure $|q\bar{q}\rangle$ ($q = up, down$ quarks) and $|s\bar{s}\rangle$ states, the latter is due to the color confining interaction. Therefore, in order to make a closer description of physical mesons like the pseudoscalars η and η' or the vector ω and ϕ mesons, a flavor mixing (FM) should be implemented.

Meson	$\{J^P, (0,0)_1, Y, T\}$
Pseudoscalar	
π	$\{0^-, (0,0)_1, 0, 1\}$
K	$\{0^-, (0,0)_1, \pm 1, \frac{1}{2}\}$
η, η'	$\{0^-, (0,0)_1, 0, 0\}$+FM
Vector	
ρ	$\{1^-, (0,0)_1, 0, 1\}$
K^*	$\{1^-, (0,0)_1, \pm 1, \frac{1}{2}\}$
ω, ϕ	$\{1^-, (0,0)_1, 0, 0\}$+FM

Table 1. Identification of the collective-state-subspaces with physical mesons.

In these sample calculations, we have restricted to total single particle spin $j = \frac{1}{2}$, and take the maximal number of oscillation quanta $N_{max} = 3$. One feature we noted for this low energy calculation is that the $-\frac{a}{|\mathbf{x}-\mathbf{y}|}$ interaction does not have a big influence on the TDA and RPA results, which is due to the low energy regime where long-range ($b|\mathbf{x}-\mathbf{y}|$) effects are dominant. For higher maximal number of oscillation quanta N_{max}, the contribution of the interaction $-\frac{a}{|\mathbf{x}-\mathbf{y}|}$ becomes more important, as expected. However, when the cut-off, N_{max}, is increased, the calculations must be renormalized in order that the observables remain unchanged. The details about the renormalization of the quark masses $m_{u,d}, m_s$ and of the coupling constants a and b as a function of N_{max} are discussed in [22].

Set	$m_{u,d}[GeV]$	$m_s[GeV]$	$b[GeV^2]$
1	0.008	0.31	0.25
2	0.008	0.31	0.40

Table 2. Sets of parameters used for the TDA and RPA calculations. The a parameter is set to zero and the oscillator length $1/\sqrt{B_0}$ is fixed at 0.7 fm.

In Table 2, we show the parameters used in these sample calculations. The first set leads to a relatively heavy pion-like state while the second set leads to a pion-like state closer in energy to the experimental value. The selection of these two sets is motivated from the LGT, where one can find that the pion reported is at about 400 MeV [4] or at about 150 MeV [3]. In both case we explore how the TDA and RPA pseudoscalar and vector spectrum at about 1 GeV looks like. The results are presented in Table 3.

State	Exp.	Set-1(TDA)	Set-1(RPA)	Set-2(TDA)	Set-2(RPA)
π	139	392.8	369.3	269.2	159.7
K	495	580.1	580.1	490.5	490.5
η	547	467.0	485.2	402.1	402.3
η'	957	719.4	688.0	646.2	586.2
ρ	770	643.0	639.5	710.8	698.9
ω	782	695.9	691.3	784.5	782.6
K^*	892	852.9	852.9	966.1	966.1
ϕ	1020	1020.4	1020.4	1144.5	1135.5

Table 3. Comparison of pseudoscalar and vector mesons with the TDA and RPA results obtained using Sets 1 and 2 of parameters.

The two set of parameters of Table 1 are able to reproduce relatively well the meson spectrum at low energy. In the case of Set-1, the pion state is higher in energy compared to the experimental value, but the rest of the collective pseudoscalar and vector mesons are in good agreement with data. In the case of Set-2, the mass of the RPA pion-like state is closer to the experimental value, but the pseudoscalar states associated with $Y, T = 0, 0$ are lowered in energy. The latter is an indicator that in the present approach certain interactions are missing, *e.g.*, related with dynamical gluons. However, the present results show that observed energy differences in spin and isospin are satisfactorily reproduced, to some extent.

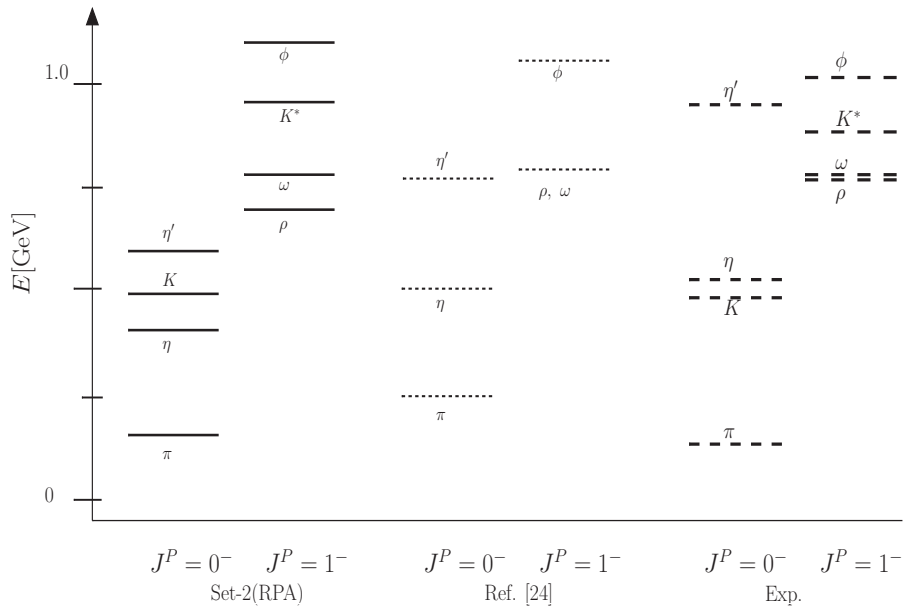

Figure 1. RPA results of Set-2 compared with experimental data and the results given in Ref. [24].

In Figure 1, we show the RPA results for Set-2 and compare them with experimental values and the results of similar approaches that use free trial wave functions.

5. Conclusions and Discussion.

We have presented a motivated QCD Hamiltonian which considers a realistic confining interaction, and used the harmonic oscillator as a trial wave functions to describe the extension of the fermion fields. We presented the exact diagonalization of the kinetic energy which provides the effective basis used for the implementation of the TDA and RPA many body methods for the diagonalization of the motivated QCD Hamiltonian.

Noticing that the $-\frac{a}{|\mathbf{x}-\mathbf{y}|}$ contribution does not modify sensibly the results at low energy, we use only the linear interaction $b|\mathbf{x}-\mathbf{y}|$ in order to investigate the low energy spectrum of pseudoscalar and vector mesons. However, the sample calculations presented here correspond to a low energy cut-off. The general case with an arbitrary cut-off, requires the renormalization of the quark masses and couplings of the interactions [22].

The TDA and RPA results indicate a pattern which resembles several features of the low energy meson spectrum but they also indicate that certain interactions, which may be related with the gluon dynamics, are missing for an even better description of the spectrum.

Acknowledgements

T. Y-M and O. C. thank to CONICET for financial support. D.A. A-Q and P. O. H thank to CONACyT (project No. 251817) and PAPIIT-DGAPA (IN100315) for financial support.

References

[1] G.S. Bali *et al* (UKQCD Collaboration), Phys. Lett. B **309**, 378 (1993).
[2] Colin J. Morningstar and Mike Peardon, Phys. Rev. D **82**, 034507 (2010).
[3] W. Bietenholz, Int. J. Mod. Phys. E **25**, 1642008 (2016).
[4] J. Dudek, Phys. Rev. D**84**, 074023 (2011).
[5] Craig D. Roberts and Anthony G. Williams, Prog. Part. NucL Phys., **33**, 477 (1994)

[6] Reinhard Alkofer and Lorenz von Smekal Phys. Rep. **353**, 281465 (2001).
[7] M. S. Bhagwat, M. A. Pichowsky, C. D. Roberts and P. C. Tandy, Phys. Rev. C **68**, 015203 (2003).
[8] A. Chodos, R. L. Jaffe, K. Johnson y C. B. Thorn, Phys. Rev. D, 10, 2599, (1974).
[9] T. DeGrand, R. L. Jaffe, K. Johndon and J. Kiskis, Phys. Rev. D, 12, 2060, (1975).
[10] A. Szczepaniak, E. S. Swanson, C-R. Ji, and S. R. Cotanch, Phys. Rev. Lett. **76**, 2011 (1996).
[11] Peter O. Hess and Adam P. Szczepaniak, Phys. Rev. C **73**, 025201 (2006).
[12] T. D. Lee, *Particle Physics and Introduction to Field Theory*, (World Scientific, Singapue, 1981).
[13] K.J. Juge, J. Kuti, and C.J. Morningstar, Nucl. Phys. B (Proc. Suppl.) **63**, 326 (1998).
[14] A. P. Szczepaniak and E. S. Swanson, Phys. Rev. D **65**, 025012 (2001).
[15] C. Feuchter and H. Reinhardt, Phys. Rev. D **70**, 105021 (2004).
[16] D. Epple, H. Reinhardt, and W. Schleifenbaum, Phys. Rev. D **75**, 045011 (2007).
[17] T. Yépez-Martínez, P. O. Hess, A. P. Szczepaniak and O. Civitarese, Phys. Rev. C**81**, 045204 (2010).
[18] T. Yépez-Martínez *et al*, Int. J. Mod. Phys. E**20**, 192199 (2011) .
[19] T. Yepez-Martinez, D. A. Amor Quiroz, P. O. Hess and O. Civitarese, J. Phys. Conf. Ser. 730, 012020 (2016).
[20] T. Yepez-Martinez, O. Civitarese, P. O. Hess Int. J. Mod. Phys. E **25**, 1650067 (2016).
[21] T. Yepez-Martinez, O. Civitarese, P. O. Hess Int. J. Mod. Phys. E **26**, 1750012 (2017).
[22] A. Amor-Quiroz, P. O. Hess, T. Yépez-Martínez, O. Civitarese and A. Weber (to be published).
[23] P. Ring, P. Schuck, *The Nuclear Many Body Problem*, (Springer, Heidelberg, 1980).
[24] F. J. Llanes-Estrada and S. R. Cotanch, Phys. Rev. Lett. **84**, 1102 (2000).
[25] C. Patrignani et al. (Particle Data Group), Chin. Phys. C, **40**, 100001 (2016).
[26] M. Moshinsky, Nucl. Phys. **13**, 104 (1959).
[27] G.P. Kamuntavicius *et al*, Nucl. Phys. A **695**, 191 (2001).
[28] J. Escher and J. P. Draayer, J. Math. Phys. **39**, 5123 (1998).